

An application of Regge calculus to axisymmetric initial data

A.P. Gentle and L.C. Brewin

*Department of Mathematics, Monash University,
Clayton, Vic., 3168, Australia.*

Abstract

Regge calculus, a simplicial approximation to General Relativity, is used to construct initial data for several non-rotating axisymmetric spacetimes at a moment of time symmetry. In particular, axisymmetric Brill wave and black hole initial data are presented, following on from the work of Dubal. Regge initial data for a combined black hole plus radiation spacetime is also constructed, and comparison of the Regge results with recent work by Bernstein is encouraging.

1. Introduction

Regge calculus [1] is an approximation to General Relativity which replaces the smooth manifold with a lattice of simplicial blocks. It has been used successfully in a variety of highly symmetric test problems, including the construction of initial data for black hole spacetimes [2],[3], and the evolution of such data [4]. See Williams and Tuckey [5] for a recent review.

If Regge calculus is to become an accepted tool in numerical relativity, it is vital that it be tested in spacetimes with less constrictive symmetries, and the results compared to those of other numerical techniques. In this work we use Regge calculus to construct initial data for several non-rotating axisymmetric spacetimes at a moment of time symmetry, as a prelude to the full evolution problem.

We begin with a short survey of the important results from the continuum theory, and then construct a Regge lattice suitable for the study of pure Brill wave initial data, similar to the work of Dubal [6]. The convergence properties of our axisymmetric lattice are then investigated in the special case of spherically symmetric black hole boundary conditions, and finally initial data for the combined Brill wave plus black hole spacetime is constructed at a moment of time symmetry.

Standard finite-difference techniques have been used to study pure Brill wave spacetimes by both Eppley [7], Miyama [8], and Dubal [6], where the results were directly compared to finite difference solutions. The Brill wave plus black hole spacetime has been extensively investigated by Bernstein [9].

2. Continuum Initial Value Problem

At a moment of time symmetry the Hamiltonian constraint reduces to

$$^{(3)}R = 0,$$

where $^{(3)}R$ is the intrinsic curvature of the spacelike hypersurface. We choose to use the axisymmetric gravitational wave spacetime suggested by Brill [10],

$$\widetilde{ds}^2 = e^{2q(\rho,z)} (d\rho^2 + dz^2) + \rho^2 d\phi^2,$$

where the arbitrary function $q(r, z)$ can be considered the distribution of gravitational wave amplitude [11]. It is not entirely arbitrary, however, as it must satisfy the boundary conditions

$$\begin{aligned} q(0, z) = 0, \quad q_r(0, z) &= 0, \\ \text{and} \quad q_z(\rho, 0) &= 0, \end{aligned}$$

so that the hypersurface has an asymptotically well defined mass.

The standard technique for constructing initial data is to use a conformal decomposition of the form

$$ds^2 = \psi^4(\rho, z) \widetilde{ds}^2$$

where ds^2 represents the physical metric. Applying the Hamiltonian constraint to this metric yields the linear equation

$$\nabla^2 \psi = -\frac{\psi}{8} \left(\frac{\partial^2 q}{\partial \rho^2} + \frac{\partial^2 q}{\partial z^2} \right) \quad (1)$$

which is solved for $\psi(\rho, z)$ once $q(\rho, z)$ is given.

The Brill mass of the initial slice can be expressed as

$$M = -\frac{1}{2\pi} \int_s \nabla \psi \cdot d\mathbf{S} = \frac{1}{2\pi} \int_v \left(\frac{\nabla \psi}{\psi} \right)^2 d\mathbf{V},$$

and Wheeler [11] has shown that for small amplitude waves the mass varies as the square of the amplitude.

3. The Regge Lattice

In order to capture the required symmetries, we choose to construct our lattice by aligning blocks along coordinate-ordinate axes. Although this necessitates an underlying coordinate choice, it provides results more easily interpreted in terms of standard 3+1 calculations. The disadvantage to this approach is that the blocks are not rigid even when all leg lengths are specified, so extra conditions must be imposed. This will be achieved by relating various angles in each block to the surrounding leg lengths.

Given the leg lengths (metric information) l_i , and the associated defects $\varepsilon(l_i)$ (curvature measured about the leg l_i via parallel transport), the Regge equivalent of the Hamiltonian constraint at each vertex in the lattice is [11]

$$\sum_k l_k \varepsilon_k = 0$$

where the summation is over all legs l_k which meet at the vertex.

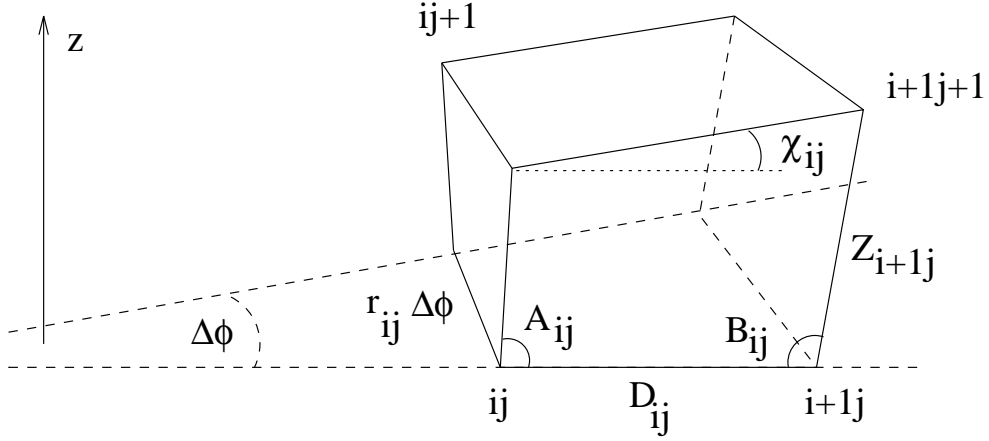


Figure 1: The generic axisymmetric block which forms the basis of the lattice, shown with respect to a global polar coordinate system.

With the choice of lattice pictured in figure (1), the Regge-Hamilton initial value equation takes the form

$$0 = 2r_{ij} \Delta\phi \varepsilon(r_{ij}) + D_{ij} \varepsilon(D_{ij}) + D_{i-1j} \varepsilon(D_{i-1j}) + Z_{ij} \varepsilon(Z_{ij}) + Z_{ij-1} \varepsilon(Z_{ij-1}) \quad (2)$$

and calculating the necessary deficit angles yields the general axisymmetric Regge initial value equation,

$$\begin{aligned} 0 = & 2r_{ij} \{A_{ij-1} - A_{ij} + B_{i-1j-1} - B_{i-1j} + \chi_{i-1j-1} - \chi_{ij-1}\} \\ + & D_{ij} \left\{ \frac{\Delta_i r_{ij}}{D_{ij}} \cot A_{ij} - \frac{\Delta_i r_{ij-1}}{D_{ij-1}} \frac{\cos(A_{ij-1} - \chi_{ij-1})}{\sin A_{ij-1}} \right. \\ & \left. - \frac{\Delta_j r_{ij}}{Z_{ij}} \frac{1}{\sin A_{ij}} + \frac{\Delta_j r_{ij-1}}{Z_{ij-1}} \frac{\cos \chi_{ij-1}}{\sin A_{ij-1}} \right\} \\ + & D_{i-1j} \left\{ \frac{\Delta_i r_{i-1j}}{D_{i-1j}} \cot A_{i-1j} \right. \\ & \left. - \frac{\Delta_i r_{i-1j-1}}{D_{i-1j-1}} \frac{\cos(A_{i-1j-1} - \chi_{i-1j-1})}{\sin A_{i-1j-1}} \right. \\ & \left. - \frac{\Delta_j r_{i-1j}}{Z_{i-1j}} \frac{1}{\sin A_{i-1j}} + \frac{\Delta_j r_{i-1j-1}}{Z_{i-1j-1}} \frac{\cos \chi_{i-1j-1}}{\sin A_{i-1j-1}} \right\} \end{aligned} \quad (3)$$

$$\begin{aligned}
& + Z_{ij} \left\{ \frac{\Delta_i r_{i-1j}}{D_{i-1j}} \frac{1}{\sin B_{i-1j}} - \frac{\Delta_i r_{ij}}{D_{ij}} \frac{1}{\sin A_{ij}} \right. \\
& \quad \left. + \frac{\Delta_j r_{ij}}{Z_{ij}} (\cot A_{ij} + \cot B_{i-1j}) \right\} \\
& + Z_{ij-1} \left\{ \frac{\Delta_i r_{i-1j-1}}{D_{i-1j-1}} \frac{1}{\sin B_{i-1j-1}} - \frac{\Delta_i r_{ij-1}}{D_{ij-1}} \frac{1}{\sin A_{ij-1}} \right. \\
& \quad \left. + \frac{\Delta_j r_{ij-1}}{Z_{ij-1}} (\cot A_{ij-1} + \cot B_{i-1j-1}) \right\}
\end{aligned}$$

where Δ_i and Δ_j are forward difference operators, defined as $\Delta_i r_{ij} = (r_{i+1,j} - r_{ij})$. In order to obtain this axisymmetric equation the limit as $\Delta\phi \rightarrow 0$ has been taken, with only the leading order terms retained.

Before a solution can be obtained, the angles A_{ij} , B_{ij} and χ_{ij} (see figure 1) must be related to the leg lengths D_{ij} , Z_{ij} and $r_{ij}\Delta\phi$. Our choice of lattice approximates the space with prisms rather than tetrahedra, so we must ensure that the faces of each block remain flat, otherwise diagonal legs must be introduced to divide each face into two triangles. This flatness criteria requires that the two independent normals to the face are parallel, providing the required condition relating angles and leg lengths.

In the case of Schwarzschild or Minkowski initial data, the flatness criteria on each face implies simple relations between the leg lengths and angles,

$$\cos A_{ij} = -\cos B_{ij} = -\frac{1}{2} \sin \chi_{ij} = -\frac{\Delta_i Z_{ij}}{2D_{ij}}.$$

These conditions are equivalent to demanding that the face $(Z_{ij}, r_{ij}\Delta\phi)$ and the equivalent face at $i+1, j$, $(Z_{i+1j}, r_{i+1j}\Delta\phi)$, are parallel. Since the solutions to be constructed in this paper may be viewed as small perturbations to Minkowski or Schwarzschild initial data, for simplicity we assume that the above flatness criteria are also applicable in our case.

In order to solve the initial value equation for the complete set of leg lengths, a conformal decomposition is used. As is the case in the 3+1 initial value problem, this results in a single unknown quantity, the conformal factor ψ , at each vertex. Although the resultant Regge-Hamilton equation is not linear, it is at worst weakly non-linear, as shown by Dubal [6].

If the structure of our lattice is aligned with the coordinate axes of cylindrical polars, examining the spacelike conformal Brill metric

$$ds^2 = \psi^4 \left\{ e^{2q} (d\rho^2 + dz^2) + \rho^2 d\phi^2 \right\}$$

suggests a conformal Regge decomposition of the form

$$\begin{aligned}
D_{ij} &= [\psi^2 e^q]_{i+\frac{1}{2},j} \Delta\rho_i \\
Z_{ij} &= [\psi^2 e^q]_{i,j+\frac{1}{2}} \Delta z_j \\
r_{ij} \Delta\phi &= \psi_{ij}^2 \rho_i \Delta\phi.
\end{aligned} \tag{4}$$

The notation $H_{i+\frac{1}{2},j}$ indicates that the quantity H is centered between the i, j and $i+1, j$ vertices.

Similarly, it is possible to consider the block in figure (1) as aligned with a global spherical polar coordinate system. These coordinates will simplify the application of spherically symmetric boundary conditions when investigating axisymmetric Brill waves in a black hole spacetime. In this case, the face (Z_{ij}, r_{ij}) lies at constant r_i , whereas the legs D_{ij} stretch from one such face to the next, and it should be noted that the labels i and j now refer to radial and azimuthal coordinates.

Using such coordinates with an exponential radius defined by $r = ae^\eta$, the Brill metric may be written in the form

$$ds^2 = \psi^4 \left\{ e^{2q} (d\eta^2 + d\theta^2) + \sin^2 \theta d\phi^2 \right\}.$$

Again comparing this with the Regge legs aligned along each coordinate axis we make a Regge conformal transformation of the form

$$\begin{aligned} D_{ij} &= \left[\psi^2 e^q \right]_{i+\frac{1}{2},j} \Delta\eta_i \\ Z_{ij} &= \left[\psi^2 e^q \right]_{i,j+\frac{1}{2}} \Delta\theta_j \\ r_{ij} \Delta\phi &= \psi_{ij}^2 \sin \theta_j \Delta\phi. \end{aligned} \tag{5}$$

In order to solve the Regge initial value problem in a particular instance, a choice of coordinate construction must be made, and the relevant expressions (4) or (5) are used in the axisymmetric Regge-Hamiltonian constraint (3). The resultant equation is solved for ψ_{ij}^2 at each vertex using Newton-Raphson iteration, given appropriate boundary conditions and the form of the function q . The initial guess was taken to be $\psi = 1$.

4. Brill wave solution

In this section we apply the Regge lattice (4), based on cylindrical polar coordinates, to reproduce the Brill wave solutions obtained via finite differencing by Eppley [7] and the Regge Calculus results of Dubal [6].

To allow comparison we choose the form of $q(\rho, z)$ given by Eppley,

$$q = \frac{A\rho^2}{1 + R^n} \quad \text{where} \quad R^2 = \rho^2 + z^2.$$

The boundary conditions on q given above imply that $n \geq 5$, and the boundary conditions on ψ are of the form

$$\begin{aligned} \frac{\partial\psi}{\partial\rho}(0, z) &= 0, & \frac{\partial\psi}{\partial z}(\rho, 0) &= 0, \\ \text{and } \frac{\partial\psi}{\partial R} &= \frac{1-\psi}{R} \quad \text{as } R \rightarrow \infty. \end{aligned}$$

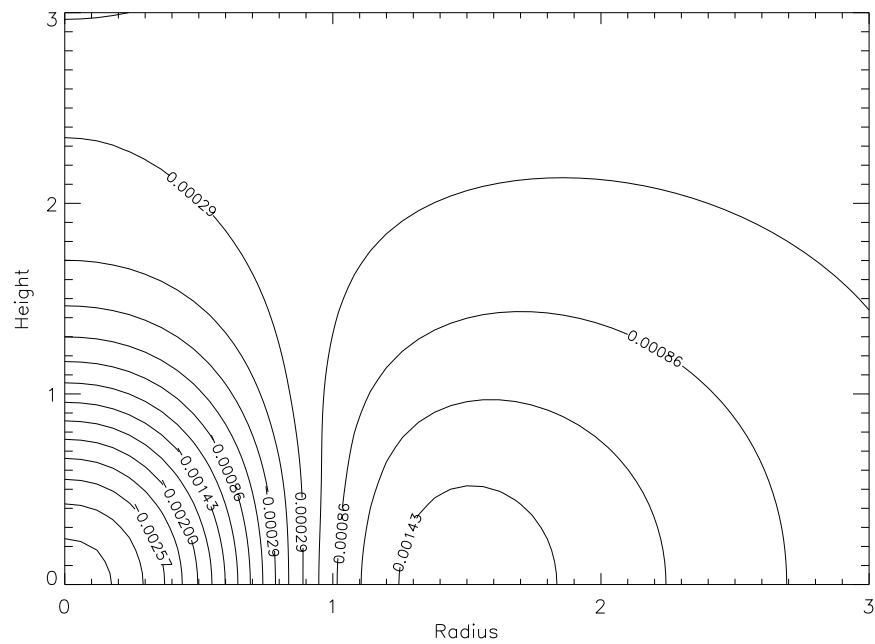


Figure 2: Perturbations from flatness, $\psi^2 e^q - 1$, for pure Brill waves with $A = 0.01$, $n = 5$ on a 50×50 grid.

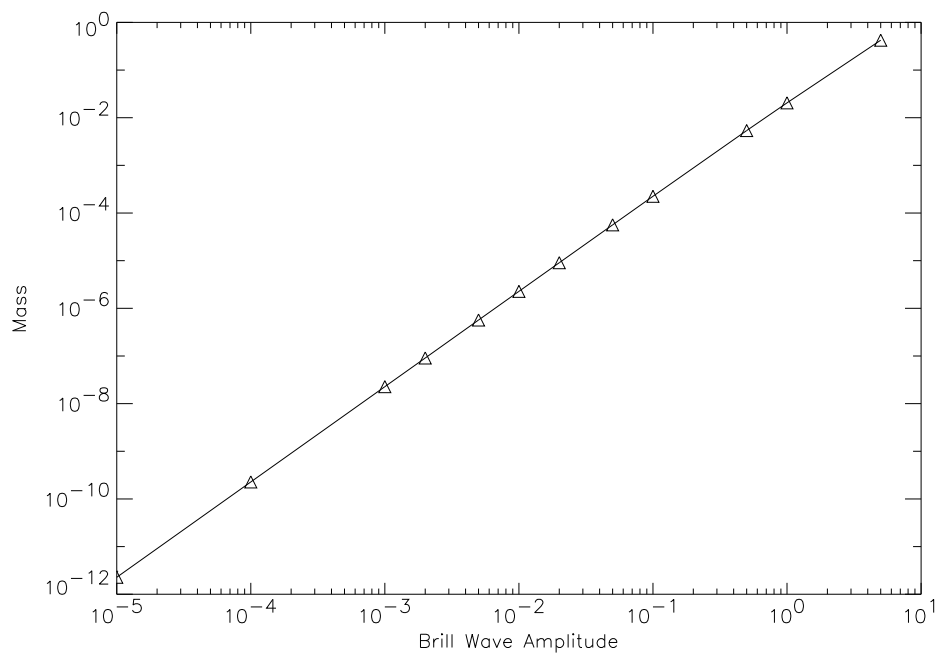


Figure 3: Mass of the pure Brill wave space plotted against amplitude of the wave on a 50×50 grid with $n = 5$.

The inner and reflection boundary conditions are implemented via a quadratic power series expansion into the domain, whereas the outer Robin boundary condition is applied to the Regge quantities ψ_{ij} via standard centered differencing.

Following Dubal, define the metric perturbation as

$$\gamma_{\rho\rho} - 1 = \psi^2 e^q - 1,$$

which may be viewed as the maximum fractional displacement of nearby observers by the passage of the wave. The perturbation is plotted in Figure (2) for a small amplitude wave with $A = 0.01$ and $n = 5$ on a 50×50 grid. As would be expected from the form of $q(\rho, z)$, the perturbations are located close to the axis of symmetry, and centered about the equatorial plane. These results agree well with the previous Regge and finite difference calculations by Dubal [6].

Finally, figure (3) shows the variation of $\log m$ with $\log A$, using the same resolution as before, which indicates that the mass varies as the square of the Brill wave amplitude, as expected.

5. Black Hole Initial Data

As a further test of the axisymmetric code, spherically symmetric boundary conditions are applied and the solution is compared with the Schwarzschild black hole. The convergence rate of the Regge model can also be calculated using this exact solution of the vacuum Einstein field equations.

In order to apply such boundary conditions, it is convenient to choose a lattice aligned with spherical polar coordinates. The conformal decomposition (5) is used, together with $q(\eta, \theta) = 0$ and inner boundary conditions of the form

$$\frac{\partial\psi}{\partial\eta}(0, \theta) = 0, \quad \frac{\partial\psi}{\partial\theta}(\eta, 0) = 0, \quad \frac{\partial\psi}{\partial\theta}(\eta, \frac{\pi}{2}) = 0,$$

where $\eta = 0$ corresponds to an Einstein-Rosen bridge at $r = a = m/2$. Again we choose to use a standard Robin condition at the outer boundary,

$$\frac{\partial\psi}{\partial r}(r_n, \theta) = \frac{1 - \psi}{r_n}.$$

where $r_n = ae^{\eta_n}$ is the radial coordinate of the outer boundary. The corresponding exact solution is

$$\psi_{bh} = \sqrt{2m} \cosh(\eta/2),$$

and in order to calculate the relative error e_n in our numerical solution on an $n \times n$ grid, define

$$e_n = \frac{1}{n} \left| \sum_{i,j} \left\{ \frac{\psi_{ij} - \psi_{bh}(ij)}{\psi_{av}} \right\}^2 \right|^{\frac{1}{2}}$$

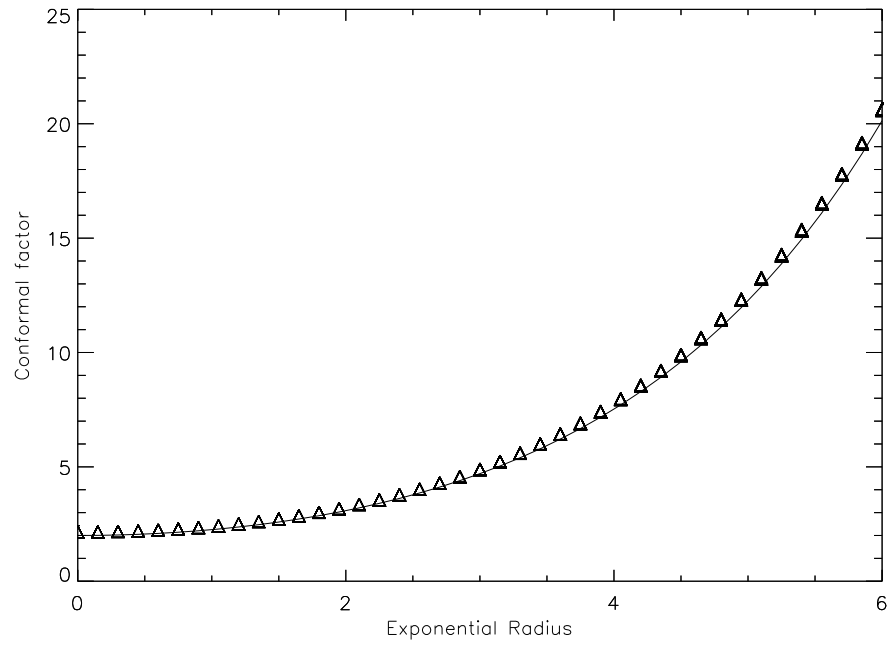


Figure 4: Regge black hole solution (triangles) against exact solution (solid line) for the case $m = 2$ on a 50×50 grid.

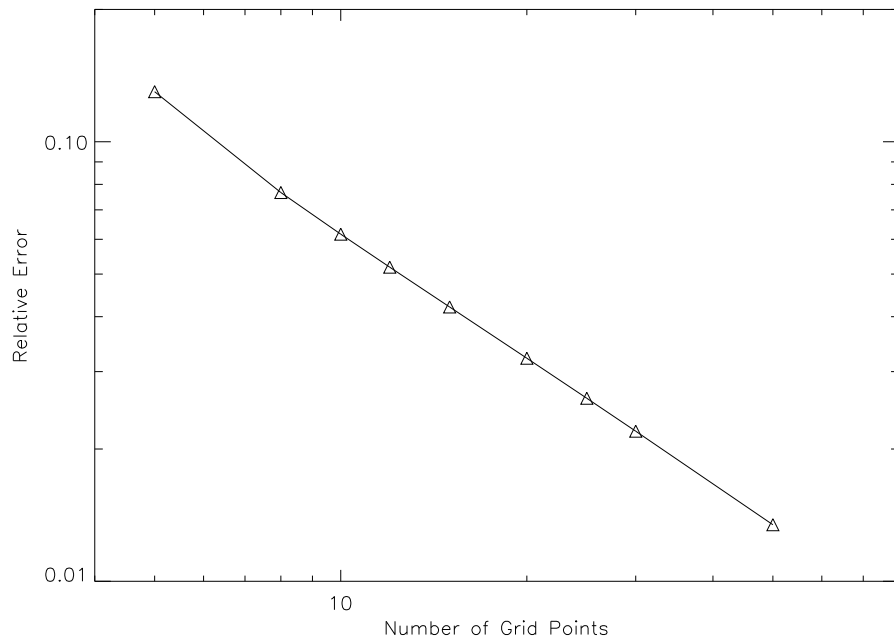


Figure 5: Relative error ϵ_n in black hole solution ($m = 2$) on an $n \times n$ grid.

where ψ_{ij} is the Regge solution at the vertex ij , $\psi_{bh}(ij)$ is the exact solution evaluated at ij , and ψ_{av} is the average value of ψ across the grid.

The solution for ψ_{ij} and the corresponding convergence rate are plotted in figures (4) and (5) respectively. It is clear that although the relative error is quite small, the convergence rate is only first order in the grid spacing.

6. Brill wave plus black hole solution

Using the spherical lattice, based on equations (5), we investigate the initial data of Bernstein [9], which contains Brill wave perturbations on a black hole spacetime. Following Bernstein, we choose $q(\eta, \theta)$ to be of the form

$$q = a \sin^2 \theta \left\{ e^{-g_+^2} + e^{-g_-^2} \right\}$$

with $g_{\pm} = (\eta \pm b)/\omega$, which contains the set of free parameters (a, b, ω) .

The boundary conditions in this case are identical to those used in the pure black hole space described above, with a reflection symmetric Einstein-Rosen bridge at $r = m/2$.

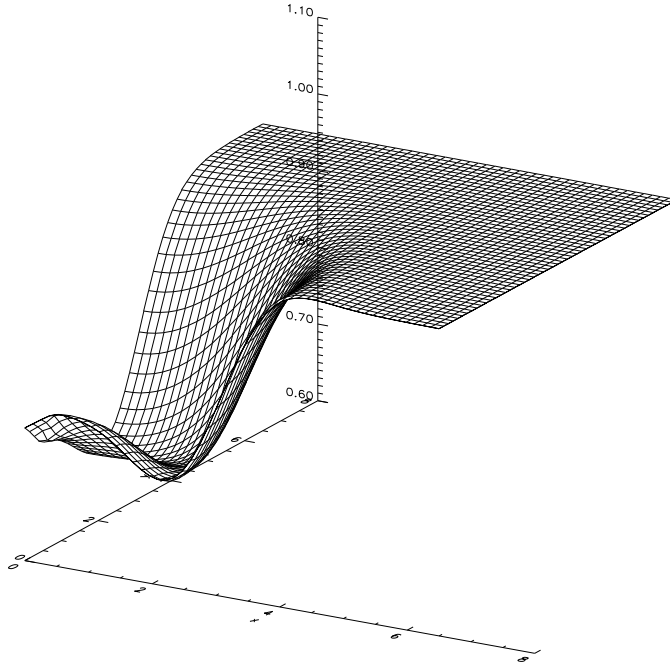


Figure 6: Ratio of Black hole plus Brill wave data to black hole initial data (ψ/ψ_{bh}) with parameters $(1, 2, 1)$ on a 50×50 grid.

For the particular choice of parameters $(1, 2, 1)$, figure (6) displays the solution to the Regge-Hamiltonian constraint (3) as ψ/ψ_{bh} , the ratio of the black hole plus Brill wave solution to the pure black hole solution of the previous section. The Regge calculations were performed on a 50×50 grid with $m = 2$, and the outer boundary was placed at

$\eta = 6$. Figure (6) is plotted on a pseudo-cartesian grid defined using $x = (\eta + \eta_0) \sin \theta$ and $y = (\eta + \eta_0) \cos \theta$, where $\eta_0 = \frac{1}{2}$ is used to display an artificial throat in (η, θ) coordinates.

These results compare well with the initial data of Bernstein [9], calculated using a second order finite-difference approximation to the Hamiltonian constraint (1).

7. Conclusions

Comparison of the Regge results with the standard finite difference calculations of Eppley [7] and Dubal [6] in the case of pure Brill radiation, and Bernstein [9] in the black hole plus Brill wave spacetime, is encouraging. The Regge Calculus solutions display features similar to those of the finite difference and analytic solutions, although further investigation of the Regge scheme's convergence rate is needed.

Previous work [12] has shown that the spherically symmetric lattice used by Wong [2] to model black hole initial data converges as the second power of the radial grid spacing, whereas our axisymmetric code displays only first order convergence when specialised to spherically symmetric boundary conditions. This disappointing convergence result may be caused by assumptions made in constructing the lattice, or may be of a more serious nature [13], [14].

It is possible that our simplifying choice for the angles A_{ij} , B_{ij} and χ_{ij} is the cause of the poor convergence rate, and so it would be worth investigating other choices. However, experience suggests that it may be more efficient to replace the prism based lattice with a full triangulation into tetrahedra. This symplectic approach may also greatly simplify the time evolution [15] of the initial data presented here.

References

- [1] T. Regge, *Nuovo Cimento* **19**, 558 (1961)
- [2] C.Y. Wong, *J. Math. Phys.* **12**, 70 (1971)
- [3] P.A. Collins and R.M. Williams, *Phys. Rev. D* **5**, 1908 (1972)
- [4] J. Porter, *Class. Quantum Grav.* **4**, 391 (1987)
- [5] R.M. Williams, P.A. Tuckey, *Class. Quantum Grav.* **9**, 1409 (1992)
- [6] M.R. Dubal, *Class. Quantum Grav.* **6**, 141 (1989)
- [7] K. Eppley *Phys. Rev. D* **16**, 6 (1977)
- [8] S.M. Miyama, *Prog. Theor. Phys.* **65**, 894 (1981)
- [9] D.H. Bernstein, *Ph.D Thesis*, University of Illinois (1993)
- [10] D.R. Brill, *Ann. Phys.* **7**, 466 (1959)

- [11] J.A. Wheeler, in *Relativity, Groups and Topology*, eds. C. DeWitt & B. DeWitt (Blackie and Son, London, 1964)
- [12] A.P. Gentle, unpublished (1994).
- [13] L.C. Brewin, gr-qc preprint #9502043 (1995)
- [14] M. Miller, gr-qc preprint #9502044 (1995)
- [15] J.W. Barrett, M. Galassi, W.A. Miller, R.D. Sorkin, P.A. Tuckey, R.M. Williams, gr-qc preprint #9411008 (1994)